JOURNAL OF APPLIED ELECTROCHEMISTRY **10** (1980) 157–168

Examination of flow models for bipolar trickle reactors

M. FLEISCHMANN, Z. IBRISAGIĆ *

Department of Chemistry, The University, Southampton, UK

Received 8 February 1978; and in revised form 23 May 1979

An electrochemical technique has been employed for determining the hydrodynamic characteristics and reaction rate constants for the bipolar trickle reactor as a whole. Theoretical descriptions of modified flow models have been derived and experimental data have been fitted to these descriptions both in the time and Laplace domains. A model with both fast and slow-moving phases gives excellent agreement with experimental curves, although a simple dispersion model is seen to be a reasonable approximation. Differences due to changes in the boundary conditions are shown to be small. The rate constant for a first order reaction has been found to be linearly dependent on the film Reynolds number, suggesting that mass transfer to the active areas within the reactor dominates the measured performance for reactions such as copper deposition.

List of symbols

A_1	extent of the fast-moving zone (cm)
A_2	extent of the slow-moving zone (cm)
C	amplitude of the response curve (arbitrary units)
C_0	tracer concentration in the fore section of the reactor (mol cm^{-3})
C_1	tracer concentration in the region where the concentration perturbation takes place (mol cm^{-3})
C_2	tracer concentration within the reactor, or in fast-moving phase (mol cm^{-3})
C_3	tracer concentration in the after section of the reactor (mol cm^{-3})
C_4	tracer concentration in the slow moving phase (mol cm^{-3})
C^0	area under the response curve for the inactive bed (mol cm^{-3} s) or initial concentration of the tracer injected over the cross-section of the reactor (mol cm^{-3})
D	dispersion coefficient ($cm^2\ s^{-1}$)
F	Faraday constant
h	film thickness (cm)
$j = 0, 1, 2 \ldots$	number of active (or inactive) zones in zoned reactor
$(j+1)b$	length of zoned reactor (cm)
$(j+1)a$	length of active part of zoned reactor (cm)
$(j+1)(b-a)$	length of inactive part of zoned reactor (cm)
J_0	Bessel function of zero order
k/h	first order reaction rate constant (s^{-1})
k'	mass transfer coefficient between fast and slow moving phases (cm s^{-1})
k_m	mass-transfer coefficient (cm s^{-1})
L	length of the reactor (cm)
n	number of electrons transferred in an electrochemical reaction
n_r	number of the rings in a single layer of packed column
(Pe)	Peclet number (uL/D)
Q	amount of tracer injected (mol)
r	reaction rate per unit area (mol $cm^{-2}\ s^{-1}$)
r_i, r_o	inner and outer radii of Raschig ring, respectively
$(Re)_f$	film Reynolds number $\left[\frac{v}{2\pi n_r(r_o + r_i)\nu}\right]$
s	Laplace variable (s^{-1})

* Present address: Banja Luka University, Faculty of Technology, 78 000 Banja Luka, Yugoslavia.

0021–891X/80/020157–12$03.20/0

S	contact area per unit length between fast and slow-moving phase
t	time (s)
$\bar{t}$	mean time (s)
u	mean liquid velocity (cm s^{-1})
v	liquid volumetric flow rate (cm^3 s^{-1})
x	spatial reactor co-ordinate (cm)
α	the parameter $\left[\left(s+\frac{u^2}{4D}\right)^{1/2}\frac{1}{D^{1/2}}\right]$
β	the parameter $\left[\left(s+\frac{k}{h}+\frac{u^2}{4D}\right)^{1/2}\right]$
γ	the parameter $u/(2D)$
Δ	region where the concentration perturbation occurs (cm)
η	electrode overpotential (V)
θ_n	roots of Equation 23
ν	kinematic viscosity (cm^2 s^{-1})
ρ	specific solution resistivity (Ω cm)
σ^2	variance (s^2)
τ	residence time (s)
ϕ_s	potential in the solution phase (V)
ω	fraction of the reactive area of a bipolar reactor (dimensionless)

1. Introduction

In the previous paper [1] we have discussed the steady state polarization behaviour of the bipolar trickle tower at a limiting condition when concentration changes in the bulk of the solution may be neglected. It was shown that for a reversible reaction this behaviour could be interpreted in terms of a one-dimensional lumped parameter model governed by

$$\frac{h}{\rho}\frac{d^2\phi_s}{dx^2} = -\frac{h}{\rho}\frac{d^2\eta}{dx^2} = -nFr \qquad (1)$$

where h is the film thickness (cm), ρ is the specific resistivity of the solution (Ω cm), ϕ_s the potential in the solution, η the overpotential, nF the number of Faradays transferred per mole of reactant and r is reaction rate per unit area (mol cm^{-2} s^{-1}).

The performance of a reactor equally depends on the mixing behaviour of the fluid elements and it is therefore important to obtain an adequate description in terms of a suitable model. In reaction engineering these models have been based either on an assembly of discrete units [2–5] (exemplified at the simplest level by a chain of perfect mixers connected by sections with plug flow) or on continuum models applied to the concentration C (mol cm^{-3}) of one species in the stream [6–12]. For example a simple one-dimensional dispersion model is described by

$$\frac{\partial C}{\partial t} = D\frac{\partial^2 C}{\partial x^2} - u\frac{\partial C}{\partial x} \qquad (2)$$

where D is the dispersion coefficient (cm^2 s^{-1}) and u is the mean liquid velocity (cm s^{-1}).* In this investigation we apply this second approach exclusively.

A particularly useful method for characterizing reactors is the tracer technique. The reactor is treated as a 'black box' and the effect of the internal mixing processes on a step or delta function concentration perturbation at the inlet is monitored at the outlet. In this paper we apply an electrochemical analogue of this method to the characterization of the bipolar trickle tower [13, 14]. The objective is the identification of a model sufficiently detailed to account for the behaviour of the reactor.

In the presence of a first order reaction, Equation 2 is modified to

$$\frac{\partial C}{\partial t} = D\frac{\partial^2 C}{\partial x^2} - u\frac{\partial C}{\partial x} - \frac{r}{h} \qquad (3)$$

$$r = kC \qquad (4)$$

where k is an appropriate rate constant (cm s^{-1}). Equation 3 is written per unit length of wetted perimeter. A major difference between conventional reaction engineering and electrochemical reaction engineering lies in the coupling of equations such as Equation 3 with Equation 1, i.e. in the distribution of reaction in space in view of the distribution of potential. Only in the case of mass transfer control throughout the reactor do these equations become uncoupled so that Equation 3 may be solved independently of Equation 1. In that case

$$k = k_m \qquad (5)$$

where k_m is the mass transfer coefficient (cm s^{-1}).

* The coefficient D arises from the random mixing of fluid elements; it includes the process of molecular diffusion but normally exceeds the diffusion coefficient by several orders of magnitude.

This case therefore is the other extreme limit as compared to that discussed in the previous papers. There has been considerable discussion in the literature [8, 16–18] concerning the correct formulation of reactor models and, indeed, of the appropriate choice of model for any particular system.

In this paper we first discuss analytical approaches to the flow modelling of electrochemical reactors (with particular attention to the modelling of the bipolar trickle system) and present data indicating the relative importance of the nature of the model and the nature of its boundary conditions. The succeeding paper presents an analysis of the reactor performance using a simple dispersion model for a wide range of operating characteristics.

2. Analysis of flow models

2.1. *Infinite flow channel*

A general specification of a reactor in an infinite channel is illustrated in Fig. 1. The delta function perturbation has usually been introduced at the boundary $x = 0$ but here we prefer to consider the perturbation as an initial condition over a short region of space $-\Delta < x < 0$. The nature of the boundary condition at $x = 0$ and the other boundary of the reactor, $x = L$, has been much discussed. It can be seen that for the model in Fig. 1 the dispersion coefficient has been assumed to be uniform throughout space and this will apply to those designs where the fore and after sections of the reactor have a packing identical to that within the reactor, i.e. an identical flow regime. The Laplace transform of the solution of the system of equations in Fig. 1 for the case $k = 0$ for the initial and boundary conditions shown may be obtained directly; at $x = L$ (the position of the detector)

$$\bar{C}_2 = \frac{C^0}{2s}\left(\frac{\alpha+\gamma}{\alpha}\right)\left[1-\exp(\gamma\text{-}\alpha)\Delta\right]\exp[(\gamma-\alpha)L] \tag{6}$$

where

$$\alpha = \left(s+\frac{u^2}{4D}\right)^{1/2}\frac{1}{D^{1/2}} \tag{7}$$

$$\gamma = \frac{u}{2D} \tag{8}$$

and s is the variable of the transformation. As $\Delta \to 0$ the perturbation takes the form of a delta function and

$$\bar{C}_2 \simeq \frac{C^0\Delta}{2s}\frac{(\alpha^2-\gamma^2)}{\alpha}\exp[(\gamma-\alpha)L] \tag{9}$$

$$= \frac{C^0\Delta}{2L} \times \frac{[(Pe)\tau]^{1/2}\exp\{(Pe)/2-[s+(Pe)/(4\tau)]^{1/2}[(Pe)\tau]^{1/2}\}}{[s+(Pe)/(4\tau)]^{1/2}} \tag{10}$$

where the Peclet number is defined by

$$(Pe) = uL/D \tag{11}$$

and the residence time by

$$\tau = L/u. \tag{12}$$

$C^0\Delta$ is the amount of material, Q, injected at $t = 0$. Equation 10 therefore inverts to

$$C_2 = \frac{Q}{2L}\left[\frac{(Pe)}{\pi(t/\tau)}\right]^{1/2}\exp\left\{\frac{-(Pe)[1-(t/\tau)]^2}{4(t/\tau)}\right\} \tag{13}$$

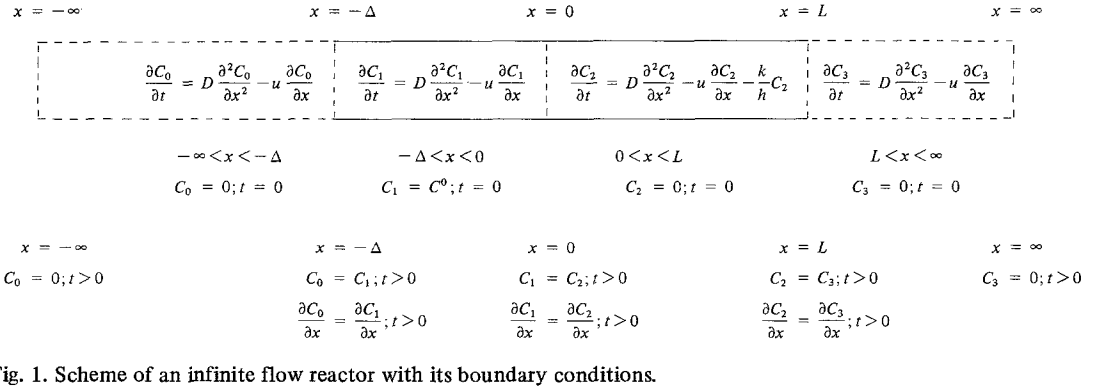

Fig. 1. Scheme of an infinite flow reactor with its boundary conditions.

an expression which has been derived in a number of ways [6, 7]. Expressions such as Equations 10 and 13 are often written in terms of the area of the transient at the outlet of the reactor. This is given by the inverse of $\bar{C}_2/s$ (or $\bar{C}_3/s$) as $s \to 0$, i.e.

$$\int_0^\infty C_2 \, dt = \frac{C^0 \Delta \tau}{L}. \tag{14}$$

Evidently

$$\frac{C^0 \Delta}{L} = \frac{Q}{L} = \frac{\int_0^\infty C_2 \, dt}{\tau} \tag{15}$$

and this is frequently written as C^0/τ in the literature.

In the presence of the reaction we obtain

$$\bar{C}_3 = \frac{C^0 \Delta}{2L} [(Pe)\tau]^{1/2} \left[s + \frac{k}{h} + \frac{(Pe)}{(4\tau)} \right]^{1/2}_{1/2} \times \exp\left[\frac{(Pe)}{2}\right] \left(\left(s + \frac{(Pe)}{4\tau} \right) \left(s + \frac{k}{h} + \frac{(Pe)}{4\tau} \right) \right)^{1/2} \times \cosh\left\{ \left[s + \frac{k}{h} + \frac{(Pe)}{4\tau} \right]^{1/2} [(Pe)\tau]^{1/2} \right\} + \left(s + \frac{k}{2h} \right) + \frac{(Pe)}{4\tau} \sinh\left\{ \left[s + \frac{k}{h} + \frac{(Pe)}{4\tau} \right]^{1/2} [(Pe)\tau]^{1/2} \right\} \Bigg)^{-1} \tag{16}$$

2.2 *Semi-infinite flow channel*

It is frequently convenient to simplify the treatment of the boundary at $x = 0$ particularly in the analysis of more complicated models of the reactor. By assuming $D = 0$ in the fore section of the reactor ($-\infty < x < 0$) we can ignore this fore section and replace the delta function perturbation by a step function

$$C_2 = C^0, x = 0, t > 0 \tag{17}$$

The response at $x = L$ to the delta function perturbation at $x = 0$ is then obtained by differentiating the solution in real time or multiplying the Laplace transform by s. Here we obtain

$$\bar{C}_2 = C^0 \exp\left\{ \frac{(Pe)}{2} - \left[s + \frac{k}{h} + \frac{(Pe)}{4\tau} \right]^{1/2} [(Pe)\tau]^{1/2} \right\} \tag{18}$$

and in real time

$$C_2 = \frac{C^0}{2\tau} \left[\frac{(Pe)}{\pi(t/\tau)^3} \right]^{1/2} \exp\left\{ \frac{-(Pe)[1-(t/\tau)]^2}{4(t/\tau)} - \frac{kt}{h} \right\} \tag{19}$$

The relative simplicity of Equation 18 as compared to Equation 16 will be evident. The validity of using this model depends on the extent to which the experimental reactor is sensitive to the exact conditions in the fore section or to the conditions within the reactor itself.

The Laplace transforms of the solutions of a number of general models where the dispersion coefficients in the fore and after sections differ from that in the reactor section have been tabulated [17]. In general it will be difficult, however, to fit the large number of parameters required by such models and here we have instead focused attention on the conditions within the reactor. A possible limiting pattern of behaviour is that when dispersion in the after section is also zero, then the boundary condition at $x = L$ may be replaced by the Danckwerts boundary condition [8]

$$\frac{\partial C_2}{\partial x} = 0, x = L, t > 0^*. \tag{20}$$

Here we obtain

$$\bar{C}_2 = \frac{C^0}{D^{1/2}} \left(s + \frac{k}{h} + \frac{u^2}{4D} \right)^{1/2} \exp\left(\frac{uL}{2D} \right) \times \left[\frac{1}{D^{1/2}} \left(s + \frac{k}{h} + \frac{u^2}{4D} \right)^{1/2} \cosh\left(s + \frac{k}{h} + \frac{u^2}{4D} \right)^{1/2} \frac{L}{D^{1/2}} + \frac{u}{2D} \sinh\left(s + \frac{k}{h} + \frac{u^2}{4D} \right)^{1/2} \frac{L}{D^{1/2}} \right]^{-1} \tag{21}$$

or

$$C_2 = 2C^0 DL \exp\left[\frac{uL}{2D} - \left(\frac{k}{h} + \frac{u^2}{4D} \right) t \right] \times \sum_{n=1}^{\infty} \left[\frac{\theta_n^3 \exp(-D\theta_n^2 t)}{\theta_n^2 L^2 + uL/(2D) + u^2 L^2/(4D^2)} \right] \sin \theta_n L \tag{22}$$

where $\pm \theta_n$ are the roots of

$$\theta_n L \cot \theta_n L + \frac{uL}{2D} = 0 \tag{23}$$

2.3. *Fast and slow moving phases*

Models in which the flow is described by a single

* This boundary condition is sometimes written in a different form but the effect is always that of 'closing the channel'.

moving 'phase' are unlikely to apply to electrochemical reactors in general, and especially so to structures such as the bipolar trickle tower. This will certainly contain regions of 'stagnant' electrolyte and at the next level of complexity we have to take into account the extents A_1 and A_2 (cm) of the fast and stagnant 'phases',† their area of contact S per unit length and the rate constant k' (cm s^{-1}) for exchange of material between these phases. For the semi-infinite channel (in the absence of reaction) we therefore solve

$$\frac{\partial C_2}{\partial t} = D\frac{\partial^2 C_2}{\partial x^2} - u\frac{\partial C_2}{\partial x} - \frac{k'S}{A_1}(C_2 - C_4) \tag{24}$$

$$\frac{dC_4}{dt} = \frac{k'S}{A_2}(C_2 - C_4) \tag{25}$$

where C_4 is the concentration in the stagnant phase. We apply the initial conditions

$$C_2 = 0, 0 < x < \infty, t = 0 \tag{26}$$

$$C_4 = 0, 0 < x < \infty, t = 0 \tag{27}$$

and obtain*

$$\bar{C}_2 = C_2^0 \exp\left\{\frac{(Pe)}{2} - \left[\frac{(k'S/A_1)\,s}{(k'S/A_2)+s} + s + \frac{(Pe)}{4\tau}\right]^{1/2} \times [(Pe)\tau]^{1/2}\right\} \tag{28}$$

Inverted forms of equations such as Equation 28 are complicated; here we obtain

$$C_2 = C_2^0 \exp\left\{\frac{(Pe)}{2} - \frac{k'St}{A_2}\right\} \times \int_0^t J_0\left[2\sqrt{\frac{k'^2S^2}{A_1A_2}y(t-y)}\right] g(y)\,dy \tag{29}$$

where J_0 is the Bessel function of zero order and $g(y)$ is determined by

$$g(y) = \frac{(Pe)}{4\pi\tau(t/\tau)^3} \exp\left\{\frac{(Pe)\tau}{4t} - \left[\frac{k'S}{A_1} - \frac{k'S}{A_2} + \frac{(Pe)}{4\tau}\right]t\right\}. \tag{30}$$

† We follow the terminology in the literature [9]; it should be noted that the two regions contain the identical electrolyte.

* For a model with the Danckwerts boundary condition at $x = L$ see [9].

For the infinite channel

$$\bar{C}_2 = (C^0\Delta/L)[(Pe)\tau]^{1/2} \exp\left\{\frac{(Pe)}{2} - \left[\frac{(k'S/A_1)\,s}{(k'S/A_2)+s} + s + \frac{(Pe)}{4\tau}\right]^{1/2} [(Pe)\tau]^{1/2}\right\} \times \left\{\left[s + \frac{(Pe)}{4\tau}\right]^{1/2} + \left[\frac{(k'S/A_1)\,s}{(k'S/A_2)+s} + s + \frac{(Pe)}{4\tau}\right]^{1/2}\right\}^{-1}. \tag{31}$$

Finally, if we allow for first order reactions with rate constants k_2/h (s^{-1}) and k_4/h (S^{-1}) in the two phases we obtain for the semi-infinite channel

$$\bar{C}_2 = C_2^0 \exp\left\{\frac{(Pe)}{2} - \left[\frac{(k'S/A_1)(s + k_4/h)}{(k'S/A_2)+s+k_4/h} + s + \frac{k_2}{h} + \frac{(Pe)}{4\tau}\right]^{1/2} \times [(Pe)\tau]^{1/2}\right\} \tag{32}$$

2.4. *Zoned reactor*

In the analysis of reactors in the presence of a first order reaction (equations such as Equation 16, 18 and 32) the rate constant k is a space-averaged quantity. In practice the distribution of potential within the reactor will produce an inhomogeneous distribution of reaction and this will be true in particular for bipolar reactors. It will be evident that the reaction rate is zero over a substantial part of the reactor and the effects of this type of inhomogeneity must be clearly distinguished from that, for example, due to regions of stagnation.

It has already been pointed out that the simultaneous solution of Equations 1 and 3 poses great difficulties. A simplified model has been applied to steady state experiments under plug flow conditions [19, 20] which takes into account the very rapid variation of the electrochemical reaction rate with potential: the reaction is assumed to be under mass transfer control over part of the surfaces of the reactor and zero elsewhere. Here we assume the simplest case: a semi-infinite channel with uniform dispersion along the axis.

The system of equations applicable to the active ($nb < x < nb + a$) and inactive ($nb + a < x < (n+1)\,b$) zones is illustrated in Fig. 2 and the set of general solutions in Fig. 3. Here

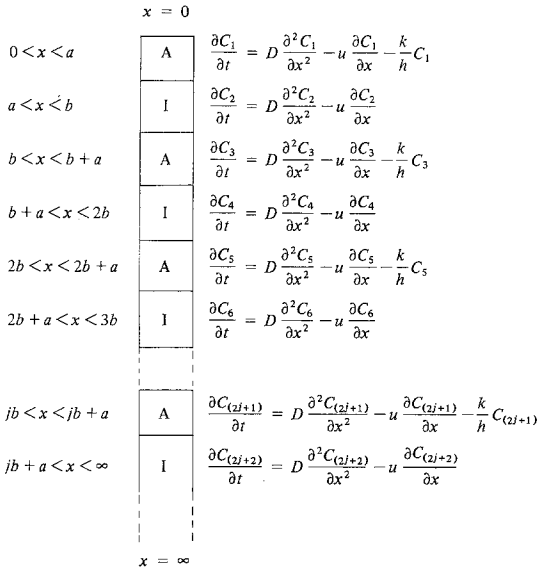

Fig. 2. Scheme of the zoned reactor. A, active zones; I, inactive zones.

$$\beta = \left(s + \frac{k}{h} + \frac{u^2}{4D}\right)^{1/2} \frac{1}{D^{1/2}}. \tag{33}$$

Fig. 3 also shows the way in which the undetermined coefficients appear in successive boundary conditions. All of these conditions can be written as an array except for the last

$$C_{(2j+2)} = 0, x = \infty, t \geqslant 0 \tag{34}$$

This condition also shows that

$$A_{(2j+2)} = 0 \tag{35}$$

and this result can be incorporated into the last two equations of the array. The general problem of seeking a solution is therefore best approached by matrix algebra; here we need the concentration at the outlet of the reactor $x = jb + a$ and therefore seek the solution for $B_{(2j+2)}$ only.

$$B_{(2j+2)} = \frac{M_{(4j+3)}}{D_{(4j+3)}}. \tag{36}$$

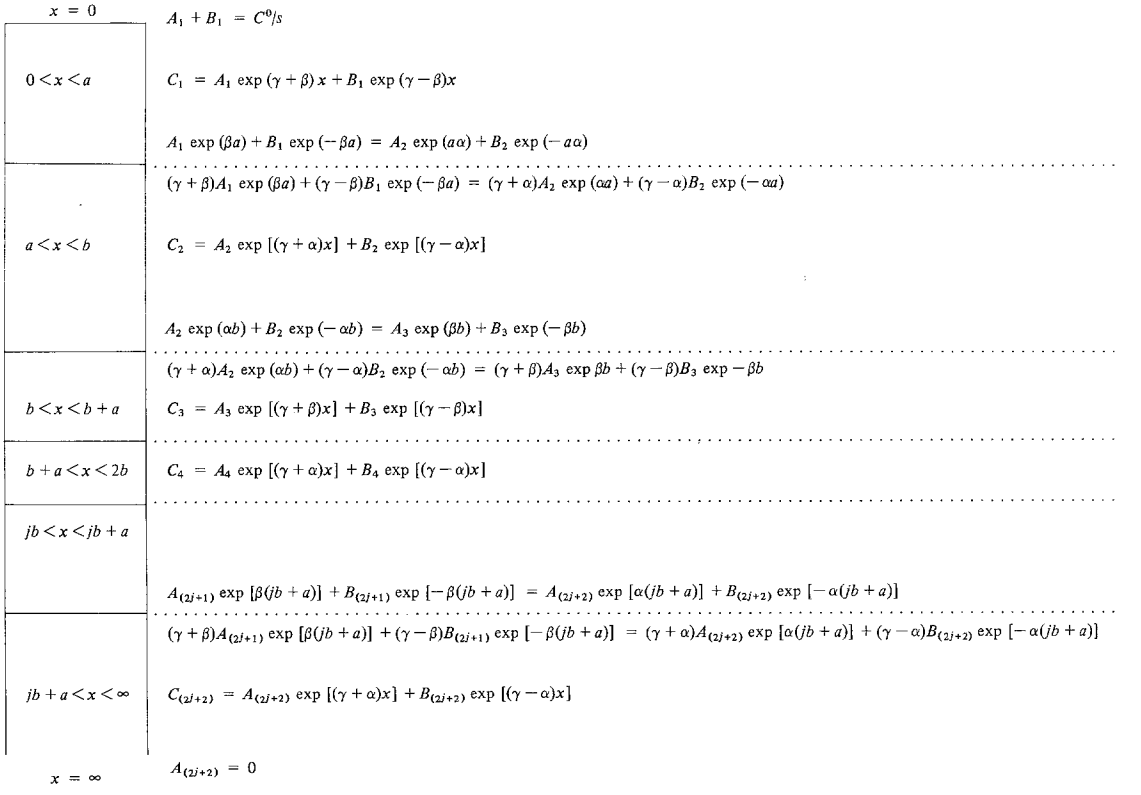

Fig. 3. Laplace transforms of the solutions for the zoned reactor together with the transforms of the boundary conditions expressing the equality of the concentrations and concentration gradients at the boundaries.

Here $j = 0, 1, 2 \ldots$ is the number of active (or inactive) units for the given reactor, M is the augmented matrix and D is the appropriate determinant. For the system of equations, Fig. 2 and Fig. 3

$$M_{4j+3} = \frac{-2C^0\beta(4\alpha\beta)^j}{s}. \tag{37}$$

The general form for D rapidly becomes highly complicated. However, for the likely values of u, D and k

$$\alpha \simeq \beta \tag{38}$$

and it is found that $D_{(4j+3)}$ is dominated by a single term

$$D_{(4j+3)} \simeq -(\alpha+\beta)^{(2j+1)} \exp\,[\beta(j+1)a] \times \times \exp\,[-\alpha(j+1)a]. \tag{39}$$

Finally, the Laplace transform of the response to a delta function is

$$\bar{C}_{(2j+2)} = \left\{ \frac{2C^0 4^j \left(s+\frac{u^2}{4D}\right)^{j/2} \frac{1}{D^{j/2}} \left(s+\frac{k}{h}+\frac{u^2}{4D}\right)^{(j+1)/2} D^{-(j+1)/2}}{\left[\left(s+\frac{u^2}{4D}\right)^{1/2}+\left(s+\frac{k}{h}+\frac{u^2}{4D}\right)^{1/2}\right]^{2j+1} D^{-(2j+1)/2}} \right\} \times \exp\frac{u}{2D}(j+1)b \exp -\left[\left(s+\frac{u^2}{4D}\right)^{1/2} \frac{(j+1)(b-a)}{D^{1/2}}\right] \times \exp -\left[\left(s+\frac{k}{h}+\frac{u^2}{4D}\right)^{1/2} \frac{(j+1)a}{D^{1/2}}\right]. \tag{40}$$

In order to simplify this expression the function before the exponentials may be expanded bearing in mind that

$$\frac{k}{h} \ll s+\frac{u^2}{4D}. \tag{41}$$

Thus

$$\frac{[s+u^2/(4D)]^{j/2}\,[s+k/h+u^2/(4D)]^{(j+1)/2}\,4^j 2}{\{[s+u^2/(4D)]^{1/2}+[s+k/h+u^2/(4D)]^{1/2}\}^{2j+1}} \simeq \frac{1+(j/2+1/2)\dfrac{k}{h[s+u^2/(4D)]}}{1+(j/2+1/4)\dfrac{k}{h[s+u^2/(4D)]}}. \tag{42}$$

This quantity remains close to unity even though $(j/2+1/2)\,k/h\,[s+u^2/(4D)]$ may not be negligible. Therefore writing $(j+1)b = L$ and

$$a/b = \omega \tag{43}$$

the fraction of active area in the reactor, we obtain

$$\bar{C} = C^0 \exp\left\{\frac{(Pe)}{2} - \left[s+\frac{(Pe)}{4\tau}\right]^{1/2} [(Pe)\tau)]^{1/2}(1-\omega) - \left[s+\frac{k}{h}+\frac{(Pe)}{4\tau}\right]^{1/2} [(Pe)\tau)]^{1/2}\,\omega\right\}. \tag{44}$$

Finally, at short times (long s) Equation 44 reduces to

$$\bar{C} = C^0 \exp\left(\frac{(Pe)}{2} - \left\{\left[s+\frac{(Pe)}{4\tau}\right]^{1/2} + \frac{k\omega}{2h\,[s+(Pe)/(4\tau)]^{1/2}}\right\} [(Pe)\tau)]^{1/2}\right) \tag{45}$$

an expression which is identical to that derived from Equation 18 provided k/h in that expression is replaced by $k\omega/h$. At the first level of approximation therefore the use of the semi-infinite model leads to values of the rate constant scaled by the fraction of the active area.

3. Experimental

The experiments were performed in the bipolar trickle tower illustrated in Fig. 1 of the previous paper [1]. The length of the reactor section was 10.3 cm and this was packed with 14 layers of ¼ inch graphite Raschig rings; each layer contained 43 rings and the column diameter was 4.88 cm. The range of liquid flow rates was 200–600 cm^3 min^{-1} and measurements were made for increments in volumetric velocity of 50 cm^3 min^{-1}.

Measurements were made in 0.5 M sodium sulphate containing 10^{-3} M sulphuric acid. All the experiments have been made at room temperature with the AnalaR reagents dissolved in de-ionized water. A concentration pulse of copper ions was introduced in the entering stream across the cross-sectional area of the reactor by using additional copper electrodes shown in Fig. 1 [1]. The detector (close spaced Pt-meshes) in the exit stream was maintained in the limiting current plateau for copper deposition. Because of the discontinuity of the trickle flow, the detector section was flooded, the level of the liquid being maintained ~ 1 mm above the electrodes by using a levelling vessel.

Measurements were made for inactive beds and for active beds when sufficient voltage was applied across the reactor to lead to copper deposition on each of the bipolar layers (2 V per unit cell). Transients were either recorded directly on an X–Y recorder or acquired on-line to a PDP-11-50 computer via a Tektronix 4010-10 terminal. Data analysis was carried out with the same machine.

4. Results and discussion

Fig. 4 shows two typical responses, one for an inactive (I) and one for an active (A) bipolar trickle reactor. It can be seen that there is considerable tailing as compared to the response which would be predicted for the simple semi-infinite or infinite channel models (Equations 13 and 19) and this immediately suggests the presence of the 'dead zones' of a slow moving phase. Data such as those in Fig. 4 have frequently been analysed by evaluating the moments of the curves [12]. This method has the advantage of leading to simple expressions for each model and moreover does not require the inversion of the transform since

$$-\left(\frac{\mathrm{d}\bar{C}}{\mathrm{d}s}\right)_{s\to 0} = \frac{\int_0^\infty tC(t)\mathrm{d}t}{\int_0^\infty C(t)\mathrm{d}t} = \bar{t} \qquad (46)$$

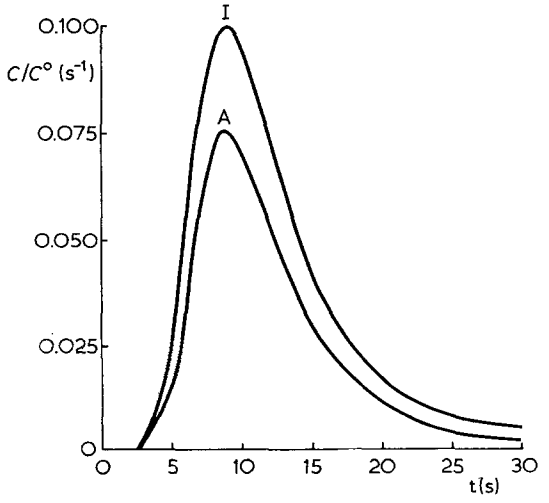

Fig. 4. Experimental response curves for an inactive (I) and an active (A) bipolar trickle reactor. C amplitude of the response; C^0 area under the response curve for the inactive bed.

and

$$\left(\frac{\mathrm{d}^2\bar{C}}{\mathrm{d}s^2}\right)_{s\to 0} - \left(\frac{\mathrm{d}\bar{C}}{\mathrm{d}s}\right)^2_{s\to 0} = \frac{\int_0^\infty t^2C(t)\mathrm{d}t}{\int_0^\infty C(t)\mathrm{d}t} - \bar{t}^2 = \sigma^2. \qquad (47)$$

However this method is subject to considerable error when there is tailing (such as in short packed beds and reactors with trickle flow, etc.). For this reason we have used non-linear regression methods throughout this investigation, the judgement for successive refinement of the parameters being based on the minimization of the standard error of fit. Fig. 5a and b show one experimental transient compared to the best achievable fit for the semi-infinite and infinite dispersion models, Equations 19 (setting $k = 0$) and 13.

The tailing will again be apparent and this is clearly inconsistent with the use of such models. Fig. 6a and b give derived data of the Peclet number (Pe) and residence time (τ) as a function of the film Reynolds number $(Re)_f$.

It can be seen that the data are not very sensitive to the nature of the boundary conditions, that is, the behaviour is dominated by the mixing within the reactor. Fig. 5c shows the fit of an experimental transient for the active bed to Equation 19 and Fig. 7 shows that the rate constant increases strongly with $(Re)_f$ indicating the importance of mass transfer control in active parts of bipolar structure. The data again are not strongly dependent on the boundary conditions.

For more complicated models fitting procedures to the data in real time are hardly feasible in view of the excessive amount of computation required. In these cases it is preferable to Laplace transform the experimental transient and fit this directly to the Laplace transform of the solution required. Numerical inversions of the transform may be carried out with the particular values. The need for this procedure can be seen by comparing Equations 29 and 30 with Equation 28. Fig. 8 illustrates such a fitting procedure; the fit is apparently excellent but it must be born in mind that the procedure emphasizes data at long time (short s). For this reason this method is particularly suitable in those situations where there is tailing.

Fig. 9 shows that the model based on fast and

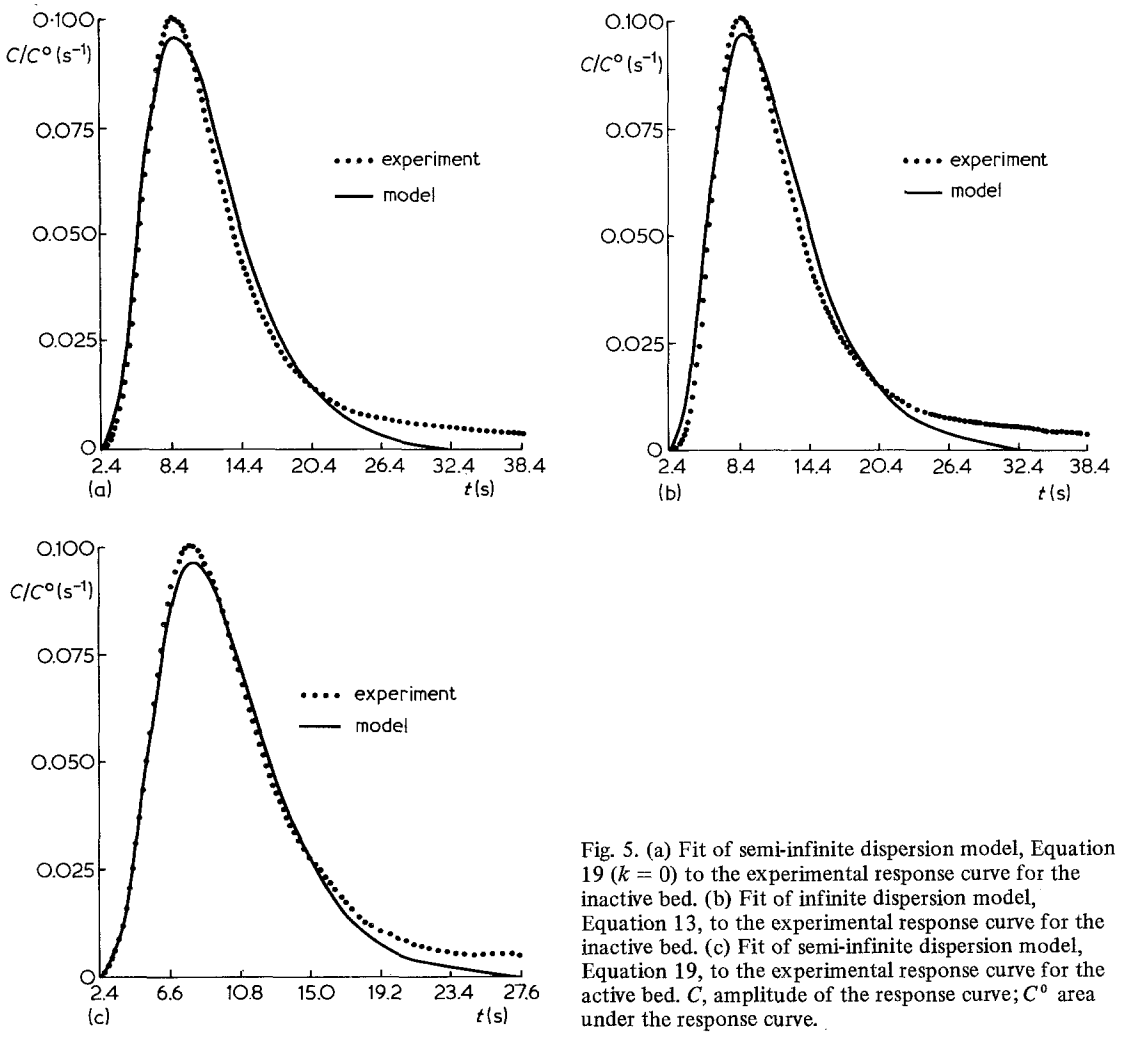

Fig. 5. (a) Fit of semi-infinite dispersion model, Equation 19 ($k = 0$) to the experimental response curve for the inactive bed. (b) Fit of infinite dispersion model, Equation 13, to the experimental response curve for the inactive bed. (c) Fit of semi-infinite dispersion model, Equation 19, to the experimental response curve for the active bed. C, amplitude of the response curve; C^0 area under the response curve.

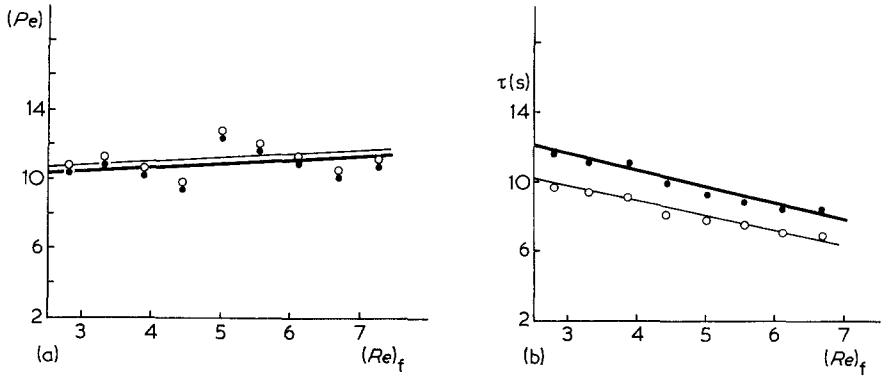

Fig. 6. Effect of boundary conditions on (Pe) and τ. (a) Relation of (Pe) to $(Re)_f$; (b) Relation of τ to $(Re)_f$. • semi-infinite, ○ infinite channel model.

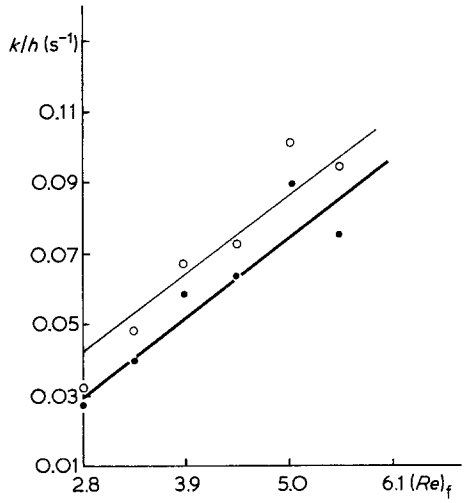

Fig. 7. Effect of boundary conditions on rate constant. Data analysis performed in the Laplace plane; Equations 16 and 18; • semi-infinite, ○ infinite channel model.

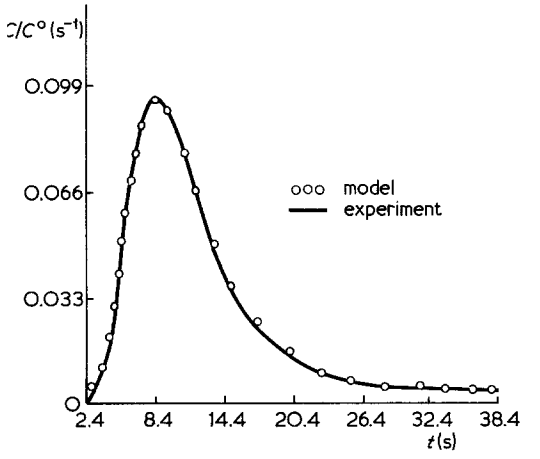

Fig. 9. Numerically inverted fit of semi-infinite model with fast and slow moving phases, Equation 28 to the experimental response curve in the Laplace plane. C amplitude of the response curve; C^0 area under the response curve; t time (s).

slow moving phases can account fully for the experimental response for trickle flow.

Figs. 10a and 10b show the derived mixing parameters as a function of $(Re)_f$. It can be seen that the extent of the fast phase is always large as compared to that of the stagnant regions and that the relative extent of the stagnant region decreases with increasing film Reynolds number. The Peclet number of the fast phase, Fig. 10b, is appreciably larger than the values derived for the semi-infinite and infinite dispersion models and the trends with increasing $(Re)_f$ are also in different senses. This is not surprising since the Peclet numbers derived from the simple dispersion models represent an average of all mixing processes such as mixing in the fast phase and exchange between fast and slow phases. It was again found that changes in the boundary conditions for this model had only minor effects; an infinite model shows slightly bigger values of $k'S/A_2$ and $k'S/A_1$.

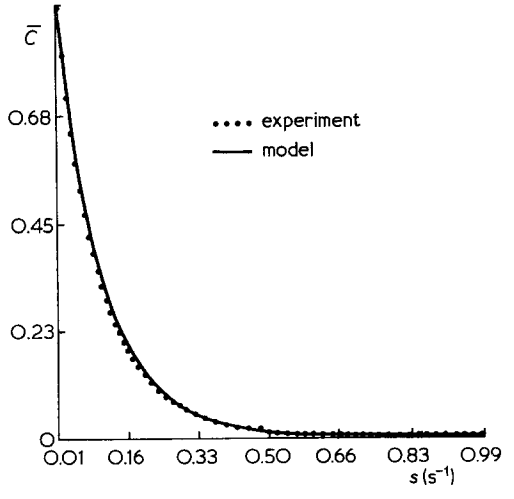

Fig. 8. Fit of semi-infinite dispersion model, Equation 19, ($k = 0$) to the experimental response curve in the Laplace plane. $\bar{C}$ amplitude of the response curve normalized by the area under the response curve and transformed into the Laplace plane; s the Laplace variable.

The rate constant k_2/h, derived for reaction in the fast moving phase, Equation 32, is found to be similar to that deduced from simple dispersion models, Fig. 7, while the rate constant k_4/h in the slow moving phase is found to be virtually zero. As the major part of the slow moving phase probably consists of the solution held by the meshes between adjacent layers of rings this indicates that reaction over the end positions of the rings does not contribute substantially to the performance of the reactor and this is in agreement with data derived in the previous paper [1] from current–potential curves. Furthermore the value of the average rate constant derived by the tracer method, i.e. $k_m = k$ at the upper limit of (Re) used in the experiments is 2×10^{-3} cm s^{-1}; the values derived from current–potential curves, extrapolated to the same value of $(Re)_f$ are $\sim 3.5 \times 10^{-3}$ cm s^{-1}. This discrepancy is probably mainly due to the fact that only part of the total area is used for the reaction. Equation 45 derived for the zoned reactor model shows that the first approximation for

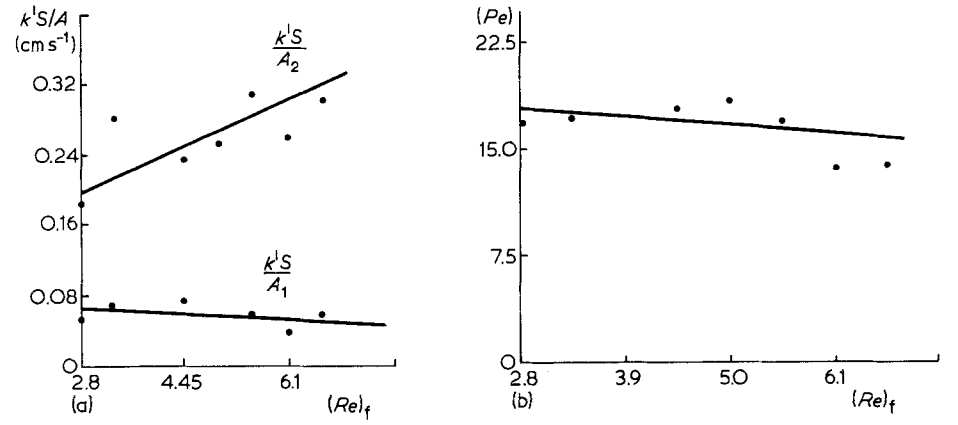

Fig. 10. Exchange between fast and slow-moving phases, Equation 28. k' mass-transfer coefficient between fast and slow-moving phases (cm s^{-1}); S contact area per unit length between fast and slow moving phases; A_1 and A_2 extents of the fast (1) and slow (2) moving phases; (b) Relation of (Pe) to $(Re)_f$, Equation 28. (Pe) the Peclet number for the fast moving phase.

the rate constant is the true value multiplied by the fraction of reactive area. The use of this equation therefore does not allow the separate evaluation of k/h and ω and even the more complete Equation 44 is not very sensitive to the separate values of k/h and ω. Fitting of this equation to the experimental data gives a rather shallow minimum in the standard error of fit for the following values of the parameter $11.16 > (Pe) > 10$, $11 < \tau < 11.16$ (s), $0.2 < \omega < 0.4$ and $0.23 > k/h > 0.11$ s^{-1}. These values of ω in turn give values of k_m which are very close to those determined from the current–potential curves and confirm that the model of the zoned reactor (in which a mass transfer controlled reaction takes place on a defined part of the reactor surface) gives an adequate description of the reactor.

5. Conclusions

It is shown that the performance of a bipolar trickle reactor may be accurately described by a lumped parameter model based on a fast- and a slow-moving phase with exchange between the phases and dispersion in the fast phase. Nevertheless simple dispersion models describe the behaviour to a first approximation. The data derived are not very sensitive to the nature of the boundary conditions chosen so that the behaviour is dominated by the reactor itself.

The extreme inhomogeneity of the reactions in these types of bipolar reactors has been described by a new zoned reactor model. This model shows that a first approximation for the reaction rate constant is the true value multiplied by the fraction of area active in the reactor. Data of the reaction rate constants derived for this model by applying the tracer method are in reasonable agreement with values deduced from current–potential curves and confirm the validity of the model.

References

[1] M. Fleischmann and Z. Ibrisagić, *J. Appl. Electrochem.* **10** (1980) 151.
[2] V. G. Levich, V. S. Markin and A. Chismadzhev, *Chem. Eng. Sci.* **22** (1967) 1357.
[3] R. W. Michell and I. A. Furzer, *Trans. Tustn. Chem. Engrs.* **50** (1972) 334.
[4] B. A. Buffham, L. G. Gibilaro and M. N. Rathor, *AICHE J.*, **16** (1970) 218.
[5] V. G. Rao and Y. B. G. Varma, *ibid* **22** (1976) 612.
[6] O. Levenspiel and W. K. Smith, *Chem. Eng. Sci.* **6** (1957) 227.
[7] O. Levenspiel, 'Chemical Reactor Engineering' 2nd edn, Wiley, London (1972).
[8] P. N. Danckwerts, *Chem. Eng. Sci.* **2** (1953) 1.
[9] J. Villermaux and W. P. M. van Swaaij, *ibid* **24** (1969) 1097.
[10] W. P. M. van Swaaij, J. C. Charpentier and J. Villermaux, *ibid* **24** (1969) 1083.
[11] A. Bennet and F. Goodridge, *Trans. Instn. Chem. Engrs.* **48** (1970) 232.
[12] R. W. Mitchell and I. A. Furzer, *Chem. Eng. J.* **4** (1972) 53.
[13] I. Justinijanović, PhD Thesis, University of Southampton (1975).
[14] Z. Ibrisagić, PhD Thesis, University of Southampton

(1977).
[15] M. Fleischmann and Z. Ibrisagić, *J. Appl. Electrochem.* **10** (1980) 169.
[16] J. F. Wehner and R. H. Wilhelm, *Chem. Eng. Sci.* **6** (1956) 89.
[17] E. Th. van der Laan, *ibid* **7** (1958) 187.
[18] D. J. Gunn, *Chem. Eng.* **CE-153** (1968).
[19] M. Fleischmann, J. W. Oldfield and C. L. K. Tennakoon, *Symposium on Electrochemical Engineering*, University of Newcastle-upon-Tyne, **1** (1971) 53.
[20] C. L. K. Tennakoon, PhD Thesis, University of Southampton (1972).